Separation Science and Technology
Publication details, including instructions for authors and subscription information:
http://www.informaworld.com/smpp/title~content=t713708471

The Enhancement of Reaction Yield Through the Use of High Temperature Membrane Reactors

T. T. Tsotsis[a]; A. M. Champagnie[a]; S. P. Vasileiadis[a]; Z. D. Ziaka[a]; R. G. Minet[a]
[a] Department of Chemical Engineering, University of Southern California, Los Angeles, California, U.S.A.

To cite this Article Tsotsis, T. T. , Champagnie, A. M. , Vasileiadis, S. P. , Ziaka, Z. D. and Minet, R. G.(1993) 'The Enhancement of Reaction Yield Through the Use of High Temperature Membrane Reactors', Separation Science and Technology, 28: 1, 397 — 422
To link to this Article: DOI: 10.1080/01496399308019497
URL: http://dx.doi.org/10.1080/01496399308019497

SEPARATION SCIENCE AND TECHNOLOGY, 28(1-3), pp. 397-422 (1993)

THE ENHANCEMENT OF REACTION YIELD THROUGH THE USE OF HIGH TEMPERATURE MEMBRANE REACTORS

T. T. Tsotsis[1], A. M. Champagnie, S. P. Vasileiadis, Z. D. Ziaka and R. G. Minet

Department of Chemical Engineering
University of Southern California
Los Angeles, California 90089-1211, U.S.A.

ABSTRACT

Membrane reactors combine reaction and separation in a single unit operation, the membrane selectively removing one or more of the reactant or product species. Most commonly these reactors have been used with reactions, whose yields are limited by thermodynamic equilibrium. For such reactions, membrane reactors seem to offer potential advantages over more traditional reactors. Membrane reactors have also been proposed for other applications; for increasing the yield of enzymatic and catalytic reactions by influencing, through the membrane, the concentration of various intermediate species; for selectively removing species, which would otherwise poison or deactivate the reaction; and for providing a controlled interface between two or more reactant species. Membrane reactors are currently being tested with a number of catalytic reactions. Reactions studied by our group include catalytic dehydrogenation of ethane, and methane steam reforming. Theoretical models have also been developed for these reactors to explain the experimental data. A brief description of our experimental and theoretical studies is presented here.

---

[1] To Whom all Correspondence Should be Addressed.

INTRODUCTION

Often catalytic reactions have yields, which are limited by thermodynamic equilibrium constraints, by low selectivities due to competitive reactions, or by slow kinetics caused by inhibition from reaction products. In many instances, these reactions prove not to be commercially feasible. Membrane reactors, which combine reaction and separation in a single unit operation, have been proposed as potential solutions for the problem of limited product yields for these reactions. In these reactors one (or more) of the product species is selectively removed from the reaction zone under the action of a permselective membrane. This in turn increases the reaction rate and often produces yields higher than the corresponding thermodynamic equilibrium yields.

The membrane reactor concept goes back over three decades. Most of the applications, however, have happened more recently due to the significant developments that have occured in the membrane materials and modules. Most of the past applications are in the field of biotechnology [1,2]. These are typically low temperature applications (<100°C) and make use primarily of porous organic/polymeric membranes but also of inorganic materials like silica or alumina, when enzyme or whole cell immobilization on such membranes appears to offer some advantage. Most recent is the use of membrane reactors in high temperature applications, typically involving catalytic processes. These reactors use metal or inorganic membranes. The membrane reactor concept as it applies to both applications is the same, but the materials considerations and emphasis are totally different.

Various membrane reactor configurations can be defined: (i) The membrane is permselective for one (or more) of the reactants and/or products. It also acts as the sole catalyst for the reaction, either itself being catalytic or impregnated with a catalyst. This configuration will be referred to as the "Catalytic Membrane Reactor", or "CMR". (ii) The membrane is catalytic and acts as the sole catalyst for the reaction. It is not permselective, however, it simply provides for a well defined interface for two (or more) reactants flowing on opposite sides of the membrane.

This configuration will be referred to as the "Catalytic Nonpermselective Membrane Reactor" or "CNMR". (iii) The membrane is permselective but not catalytic. The catalyst zone is a packed bed or fluidized bed of catalysts. These two configurations will be referred to as the packed bed (PBMR) and fluidized bed (FBMR) membrane reactors correspondingly. (iv) The membrane is catalytic and permselective. A packed or fluidized bed of catalysts also exists inside (or outside) the membrane. These two configurations will be referred to correspondingly as the packed bed (PBCMR) or fluidized bed (FBCMR) catalytic membrane reactors.

The earlier applications of high temperature catalytic membrane reactors involved the use of metallic (Pd, Pd alloy and Pd/Ag) membranes. These reactors have been pioneered by Gryaznov and coworkers who studied many hydrogenation/dehydrogenation reactions, while testing various reactors containing flat foil, thin walled straight tube and spiral-type membranes [3-9]. Pd membranes are useful because they are permeable to H_2 and virtually impermeable to other gases. Their industrial application, however, has been hindered by their low transmembrane fluxes, their high cost and associated phenomena of metal sintering, imbrittlement and fatigue. To improve on their low H_2 permeability, efforts have focused on the development of composite Pd/porous metal or Pd/ceramic membranes [10-15]. Such membranes have been used by Uemiya and coworkers for the study of the water gas shift reaction [16,17], for methane steam reforming [18,19] and for the aromatization of propane [20]. Unfortunately these composite membranes have been found to be brittle and prone to pinhole formation. Their commercialization still remains questionable in high temperature applications. Pd membranes are also prone to poisoning by sulfur, present in a number of petroleum and chemical feedstocks, and to coking. This is the most serious of problems facing the Pd membrane reactors. Sulfur or coke coverage of the surface of the Pd membranes results in significant reduction in the H_2 permeation rates.

Some successes have been reported with the use of other nonporous membrane materials, which exhibit enhanced oxygen anionic conductivity. Omata *et al.* [21] have used an Al_2O_3 porous tube coated externally with a dense MgO/PbO film in a CMR to study CH_4 oxidative coupling, with CH_4 fed in the shellside and O_2 fed in the tubeside. A 2% conversion but with over 97% selectivity was reported. O_2 conducting nonporous ceramic or metal membranes have been utilized in membrane reactors since the early seventies. Early applications involved the use of ZrO_2 and Ca-stabilized ZrO_2 membranes to decompose various O_2 containing compounds like NO, CO, CO_2 and H_2O with or without oxygen electrolytic pumping [22-26]. Yitria stabilized zirconias (YSZ) have been used by Vayenas and coworkers [27-31] for increasing the yield of various partial oxidation reactions with the aid of electrochemical oxygen pumping and by Huggins [32,33] to enhance CO and CO_2 methanation. Reactions studied by Vayenas and coworkers include C_2H_4 and propylene epoxidation, NH_3 oxidation to co-generate NO and electric energy and oxidative dehydrogenation of ethylbenzene to styrene. YSZ based membrane reactors have also been used for oxidative CH_4 coupling [34,35] and various catalytic epoxidations [36].

Dicosino *et al.* [37] report the use of bismuth oxides to carry out the oxidative dehydrodimerization of various allylic and benzylic compounds. A number of specialized materials have been tried for SO_x and NO_x and most recently H_2S decomposition [38]. Ag membranes, which also conduct O_2, have been used by Gryaznov and coworkers [39]. Oxygen anionic conductors are, of course, of greater interest in the area of solid oxide fuel cells (SOFCS), which are looked upon today as a means for replacing diesel engines for heat and power generation. SOFCS in a general sense, represent a special group of catalytic membrane reactors.

Earlier applications of catalytic microporous membrane reactors involved the use of porous glass membranes [40-43]. These membranes, however, are generally brittle and show poor resistance to thermal and mechanical stresses. High temperature catalytic reactors, using porous ceramic membranes, are a more recent development [44-52]. Earlier applications involved the use of anodic aluminas [53]. These materials are ideally suited for academic investigations of transport because they have straight nonintersecting pores [54,55]. Most recent applications have involved the use of Sol-Gel alumina, zirconia and titania membranes. A British patent by Bitter [56] claimed the use Sol-Gel alumina membranes for several dehydrogenation reactions, including the propane to propylene reaction, for which they claimed significant improvements in yield. Other studies have reported the application of catalytic reactions using Sol-Gel ceramic membranes for the dehydrogenation of methanol [48,50-52], n-butane dehydrogenation [48,51], ethylbenzene dehydrogenation to styrene [44,57] and the reaction between nitric oxide and ammonia [48].

Our group has studied the use of catalytic ceramic membrane reactors for the dehydrogenation of lower molecular weight hydrocarbons [45,46], and for methane steam reforming [47]. For the ethane dehydrogenation reaction results of our studies in a CMR have already been published [45,46]. Here we will present some results of our studies with the same reaction in a PBMR. A model for this reactor is also presented. Results of our studies of the methane steam reforming reaction in a PBMR will also be presented.

EXPERIMENTAL APPARATUS AND GENERAL DISCUSSION

Ethane Dehydrogenation

A typical example of a thermodynamically limited reaction is ethane dehydrogenation to ethylene, a valuable chemical commodity. Conversions of less than 30 percent are obtained at 700°C for pure ethane feed in a commercial ethane steam cracker. The selectivity to ethylene is 78 to 82 % with recycle, with significant amounts of by-products, such as methane, acetylene and higher hydrocarbons. Heterogeneous catalytic processes have also been developed using supported platinum on alumina catalysts, resulting in higher selectivities to ethylene of up to 98% [58]. However, the very high temperatures necessary to obtain adequate yields result in catalyst deactivation, due to metal sintering and coke formation. This reaction, therefore, is ideally suited for the application of catalytic ceramic membrane reactor technology.

The experimental apparatus used in the ethane dehydrogenation experiments is shown in Figure 1. It is also described in greater detail elsewhere [45,46]. The exper-

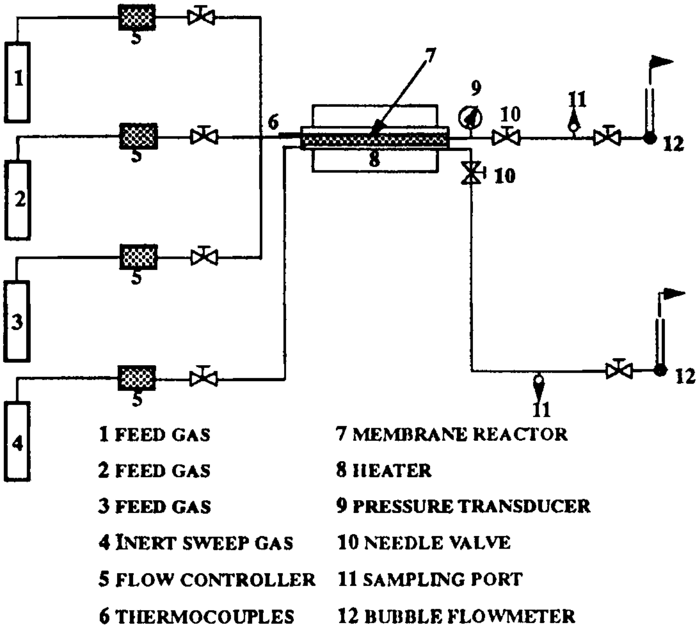

Figure 1: Schematic of Apparatus

imental system consists of the reactant gas delivery system, the high temperature membrane reactor, and the product collection and measurement devices. The multilayered composite porous alumina tube has an inner diameter of 7mm, an outer diameter of 10mm, and a length of 25cm. It is available commercially from ALCOA under the trade name Membralox^{TM} and consists of three permselective layers with pore diameters of 40Å, 2000Å and 8000Å, supported on a macroporous layer with a pore diameter of 15μm. A schematic of the 'tube-and-shell' type membrane reactor is shown in Figure 2. It consists of a stainless steel shell, with ports for the sweep gas inlet and outlet. The ceramic tube is placed inside this shell and sealed at the ends by graphite string and compression fittings. The entire reactor was operated under reasonably isothermal conditions with temperature gradients along the reactor length of less than 2°C.

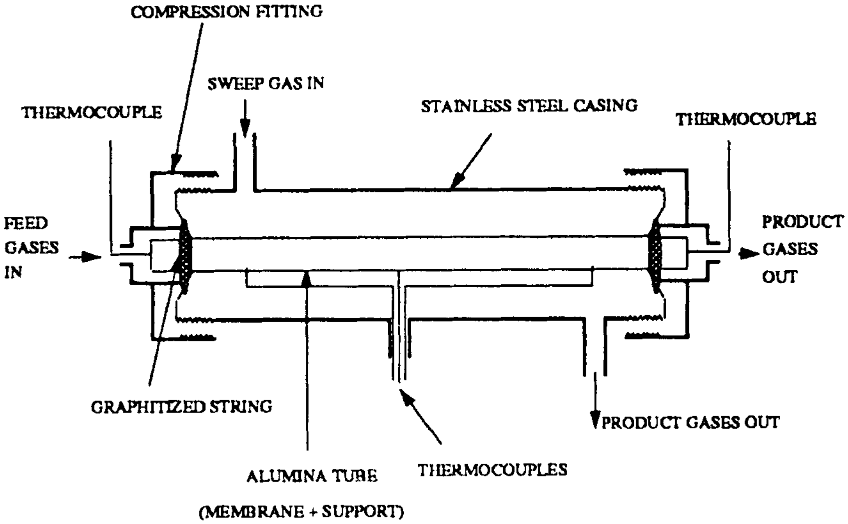

Figure 2: **Ceramic Membrane Reactor**

For the PBMR experiments, the catalyst was 3g of a commercial (Morton Thiokol) 5 wt. % Pt on alumina particles approximately 1-1.5 mm in diameter. Hydrogen was added to the ethane and argon reactant feed mixtures to prevent catalyst deactivation, due to coking. The gas stream compositions were analyzed on line using a UTI 100C mass spectrometer with an attached atmospheric pressure mass sampling unit.

Methane Steam Reforming

The methane steam reforming reaction has in the past found widespread application for hydrogen production [59]. Interest in this reaction has been recently rekindled for low temperature applications, for hydrogen production for use in chemically recuperated gas turbines and fuel cells. The temperature range of interest for these applications is 200 - 550°C. In order for the low temperature applications of methane steam reforming to be economically viable one must overcome the thermo-

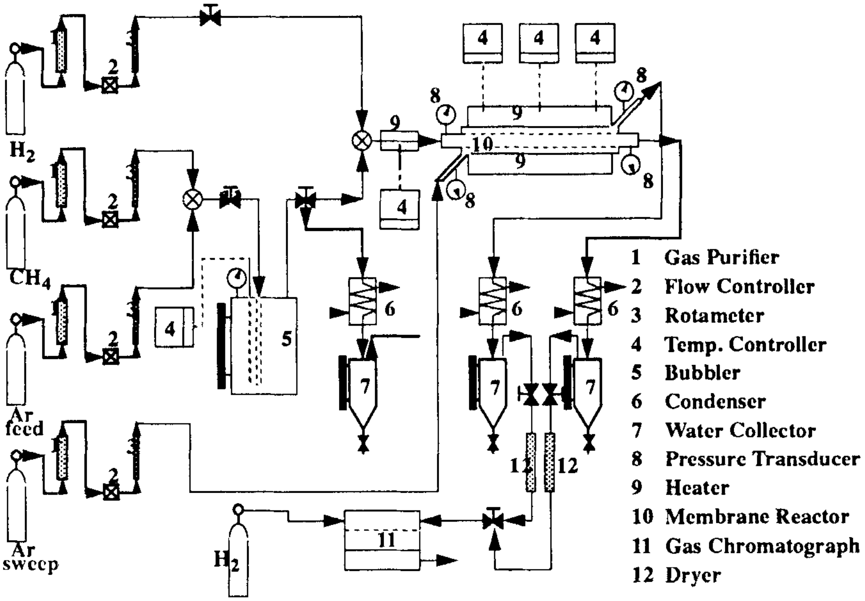

Figure 3: **Schematic of Apparatus for Methane Steam Reforming**

dynamic equilibrium limitations. This reaction is, therefore, a candidate for the application of catalytic membrane reactors. As discussed in the introduction, Uemiya and coworkers have studied this reaction in a PBMR using a Pd coated membrane [18,19]. For large space times the membrane reactor conversion exceeded the corresponding thermodynamic equilibrium. The use of Pd membranes for methane steam reforming had previously been suggested by Oertel [60] and a theoretical study of a PBMR using a Pd membrane was recently published [61]. The drawbacks with Pd membranes have already been discussed.

In our study we have utilized commercially available (Membralox^{TM}), microporous alumina membranes. The experiments reported here were performed in a PBMR in the temperature range of 445 - 590°C. The inside of the membrane was packed with commercial Ni/Al_2O_3 catalyst (15% NiO on calcium aluminate, from Katalco, Chicago IL). The catalyst was provided by the manufacturer in a cylindrical pellet configuration. These pellets were ground and 8 g of the 1 mm size fraction were placed inside the membrane.

The apparatus is shown in Figure. 3 . The flows of argon, methane and hydrogen are individually controlled and measured by mass-flow controllers. The gases are then mixed and passed through a bubbler containing water. The flow rate of the steam is controlled by means of the bubbler's temperature and pressure and measured by monitoring the drop in the liquid level inside the bubbler and the amount of water collected in the condenser. Three Omega CN2000 temperature controllers using six semi-cylindical ceramic heaters and three temperature thermocouples attached to the external membrane wall at equidistant points were used to control the temperature. The temperature of the bed of catalysts was measured by two additional thermocouples placed inside the bed. The pressure inside the reactor was adjusted with a needle valve placed on the reaction side outlet. The gases from both the reaction (tubeside) and separation (shellside) outlets are first condensed to remove the H_2O vapor, then dried and subsequently passed through the top of the collection vessels leading either to an on-line gas chromatograph with a TCD detector (3400 VARIAN) or through a bubble flowmeter.

To start an experimental run the catalyst bed was first heated slowly (2-4 °C/min) in flowing hydrogen up to a temperature of 550°C and kept at this temperature for 2 hr. Subsequently the steam flow was turned on and the reactor temperature was brought to the desired level. Once everything had stabilized, the hydrocarbon flow was initiated. For the experiments reported here the methane flow rate was kept at 0.15 gmoles/hr, the $H_2O : CH_4 : Ar : H_2$ ratios fixed at 7 : 1 : 1 : 0.75 and the temperature was varied in the range of 445 - 590°C. Argon can also be used as a sweep gas in the shellside.

Before each experimental run at a new temperature the activity of the catalyst was checked with respect to its activity at a reference temperature of 545°C. For all experiments reported here the catalytic activity was constant. The total pressure at the reaction side inlet was 2 psig, while at the outlet it was 1 psig. The shellside of the membrane was maintained at atmospheric pressures.

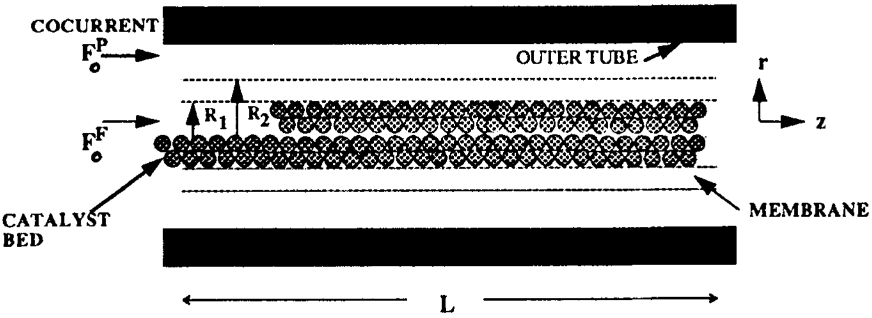

Figure 4: **Schematic of Membrane Reactor**

THEORETICAL MODEL

A theoretical model has been developed to describe the behaviour of the PBMR. A schematic of the cross-section of the reactor is shown in Figure 4. The PBMR model is based on the following assumptions:

1. The reactor is at steady state and isothermal conditions prevail. The catalyst particles, the membrane and the surrounding gas phase are all at the same temperature. The external concentration gradients between the fluid and catalytic phases are negligible.
2. Plug flow behavior prevails both in the tubeside as well as in the shellside and the radial tubeside and shellside concentration gradients are negligible. No mass transfer limitations exist between the shellside/tubeside and the membrane surface.
3. The catalyst used is packed in the tubeside, the shellside is empty. There is negligible pressure drop in the shellside. Concentration gradients in the catalyst particles are accounted for by effectiveness factors.

4. The membrane is modelled as a two layer membrane consisting of one permselective layer and a thick support layer. The mass transfer resistance in the support is negligible. Knudsen diffusion describes the transport of all gases through the membrane. Surface and bulk diffusion and convective flows are all negligible.

5. The rate for the reactions occuring in the tubeside is assumed to be of the form,

$$\mathcal{F}_i^F(C_j^F, K_{ei}'^F) = \frac{\prod_j (C_j^F)^{\beta_{ij}^f} - \prod_j (C_j^F)^{\beta_{ij}^r} / K_{ei}'^F}{G_i^F(C_j^F)} \tag{1}$$

$\beta_i^f = \sum_j \beta_{ij}^f, \beta_i^r = \sum_j \beta_{ij}^r$ being the orders of the forward and reverse reaction i correspondingly.

Based on these assumptions, the design equations for the PBMR are as follows (the various symbols are explained in the list of symbols at the end):

In the Membrane:

$$D_{je} \frac{1}{r} \frac{d}{dr} \left[r \frac{dC_j^m}{dr} \right] = 0, \tag{2}$$

where

C_j : is the concentration of species j with superscripts m, F, P signifying the membrane, feedside and permeate side correspondingly (see below),

D_{je} : is the effective Knudsen diffusivity of component j.

The boundary conditions are:

$C_j^m = C_j^F = X_j^F C_T^F$ at $r = R_1$

$C_j^m = C_j^P = X_j^P C_T^P$ at $r = R_2$,

where $C_T^F = \sum_j C_j^F$, $C_T^P = \sum_j C_j^P$ and X_j^F, X_j^P are the mole fractions of the feedside and permeate side correspondingly.

In the Tubeside:

The equation describing the tubeside is:

$$\frac{dn_j^F}{dz} = 2\pi D_{je} R_1 \left(\frac{dC_j^m}{dr}\right)_{r=R_1} + \sum_i \nu_{ij}^F \pi R_1^2 \eta_i^F k_{ri}^F \mathcal{F}_i^F (C_j^F, K_{ei}'^F) \tag{3}$$

$$n_j^F = n_{jo}^F = F_o^F C_{jo}^F \quad \text{at} \quad z = 0,$$

where n_j is the molar flowrate of component j.

The pressure drop in the tubeside can be described by a number of correlations based on relationships for fluid flow through porous media. We have used the Ergun correlation

$$-\frac{dP^F}{dz} = \frac{f\left(G^F\right)^2}{g_c d_p \rho_f}, \tag{4}$$

with:

$$f = \left(\frac{1-\epsilon^F}{\epsilon^{F3}}\right)\left[1.75 + \frac{150\left(1-\epsilon^F\right)}{N_{Re}}\right] \tag{5}$$

For the above relationship to be valid, the following condition should hold true:

$$\frac{N_{Re}}{1-\epsilon^F} < 500, \tag{6}$$

where

$$N_{Re} = \frac{d_p G^F}{\mu} \tag{7}$$

and d_p is the equivalent particle diameter. Similar relationships with (5) exist for different ranges of N_{Re} values.

In the Shellside:

$$\frac{dn_j^P}{dz} = -2\pi D_{je} R_2 \left(\frac{dC_j^m}{dr}\right)_{r=R_2} \tag{8}$$

$$n_j^P = n_{jo}^P = F_o^P C_{jo}^P \quad \text{at} \quad z = 0$$

Dimensionless quantities are defined as:

$$Y_j^m = \frac{C_j^m}{C_{To}^F},\ X_j = \frac{P_j}{P^F},\ \psi^{PF} = \frac{P_o^P}{P_o^F},\ y_j^F = \frac{n_j^F}{n_o^F},\ y_j^P = \frac{n_j^P}{n_o^F},\ \psi^F = \frac{P^F}{P_o^F},$$

$$\psi^P = \frac{P^P}{P_o^F},\quad v_j = \frac{M_j}{M_A},\ \xi = \frac{r}{R_1},\ \mathcal{D}a_i = \frac{\pi R_1^2 L k_{ri}^F C_{To}^{\beta_i^f - 1}}{F_o^F},\ \delta_j = \frac{D_{je}}{D_{Ae}},$$

$$K_{ei}^F = K_{ei}'^F C_{To}^{\beta_i^f - \beta_i^r},\ \zeta = \frac{z}{L},\ Q = \frac{2\pi D_{Ae} L}{F_o^F},\ F_r = \frac{F_o^P}{F_o^F},\ \epsilon = \frac{R_2 - R_1}{R_1},\ \omega = \frac{ln\xi}{\alpha},$$

$$\alpha = ln(1+\epsilon)$$

The dimensionless forms of Equations 2, 3 and 8 then are:

In The Membrane:

$$\frac{d^2 Y_j^m}{d\omega^2} \tag{9}$$

$$Y_j^m = X_j^F \psi^F \text{ at } \omega = 0$$

$$Y_j^m = X_j^P \psi^P \text{ at } \omega = 1$$

In the Tubeside:

$$\frac{dy_j^F}{d\zeta} = \frac{Q\delta_j}{\alpha}\left[\frac{dY_j^m}{d\omega}\right]_{\omega=0} + \sum_i \nu_{ij}^F \eta_i^F \mathcal{D}a_i \mathcal{F}_i^F (Y_j^F, K_{ei}^F) \tag{10}$$

with the initial conditions

$$y_j^F = X_{j0}^F \text{ at } \zeta = 0$$

In the Shellside:

$$\frac{dy_j^P}{d\zeta} = -\frac{Q\delta_j}{\alpha}\left[\frac{dY_j^m}{d\omega}\right]_{\omega=1} \tag{11}$$

with the initial conditions

$$y_j^P = F_r \psi^{PF} X_{j0}^P \text{ at } \zeta = 0$$

The Ergun equation becomes:

$$-\psi^F \frac{d\psi^F}{d\zeta} = \frac{f\left(\frac{F_0^F}{\pi R_1^2}\right)^2 C_{T0}^F M_A L}{g_c d_p p_0^F} \frac{\left(\sum_j y_j^F v_j\right)^2}{\left(\sum_j X_j^F v_j\right)} \tag{12}$$

with the initial condition,

$$\psi^F = 1 \text{ at } \zeta = 0$$

The above system of equations describe the PBMR for cocurrent flow conditions, i.e. when the direction of the feedside and shellside flows are the same. For

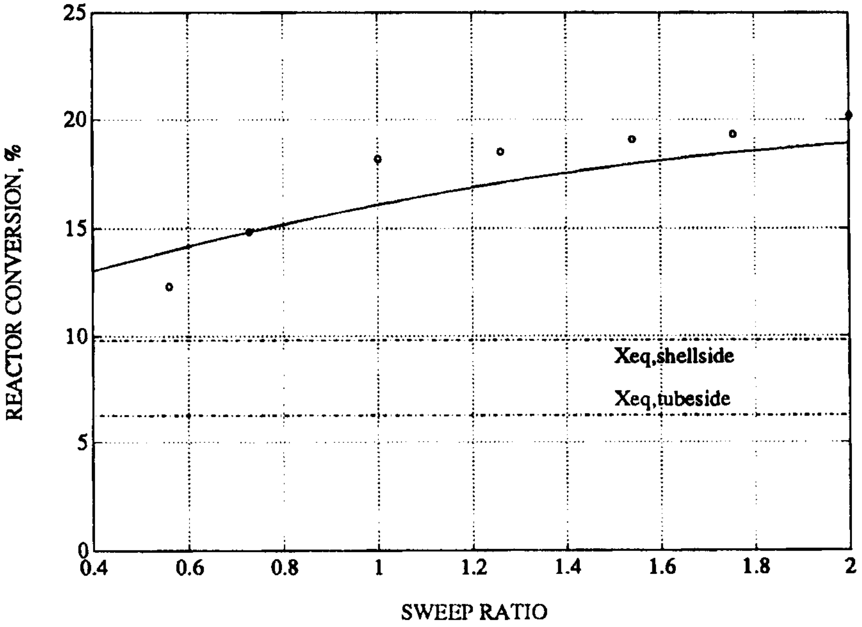

Figure 5: Conversion vs. Sweep Ratio for Dilute Feed, T = 550°C, τ = 2s, P_o^F = 30 psi, $\psi^{PF} = 0.5$

countercurrent flow configurations the shellside flow equations and conditions must be modified appropriately. Equation (9) was integrated analytically and the system of equations (10) - (12) was then integrated in a straightforward manner by a third order Runge Kutta technique. The exact numerical details can be found elsewhere [62]. The countercurrent flow problem is a split boundary value problem. Several numerical methods exist for addressing split boundary value problems of this kind.

Only one independent reaction occurs during ethane dehydrogenation, namely

$$C_2H_6 \rightleftharpoons C_2H_4 + H_2. \qquad (13)$$

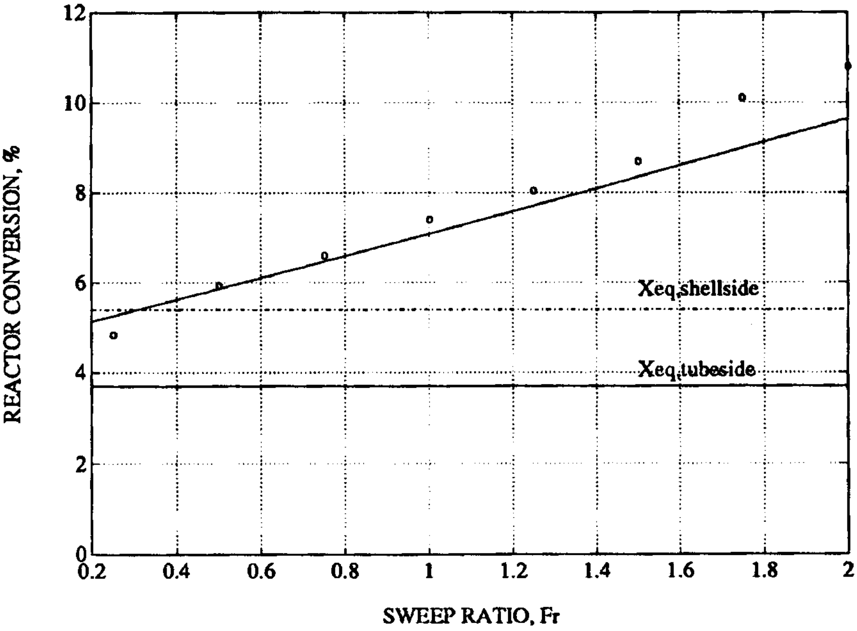

Figure 6: Conversion vs. Sweep Ratio for Dense Feed, T = 550°C, τ = 2s, P_o^F = 30 psi, $\psi^{PF} = 0.5$

On the other hand for methane steam reforming there are two independent reactions occuring namely

$$CH_4 + H_2O \rightleftharpoons CO + 3H_2 \tag{14}$$

$$CO + H_2O \rightleftharpoons CO_2 + H_2 \tag{15}$$

EXPERIMENTAL RESULTS AND DISCUSSION

Before the initiation of the membrane reactor experiments detailed kinetic investigations were performed by standard techniques in order to derive the various

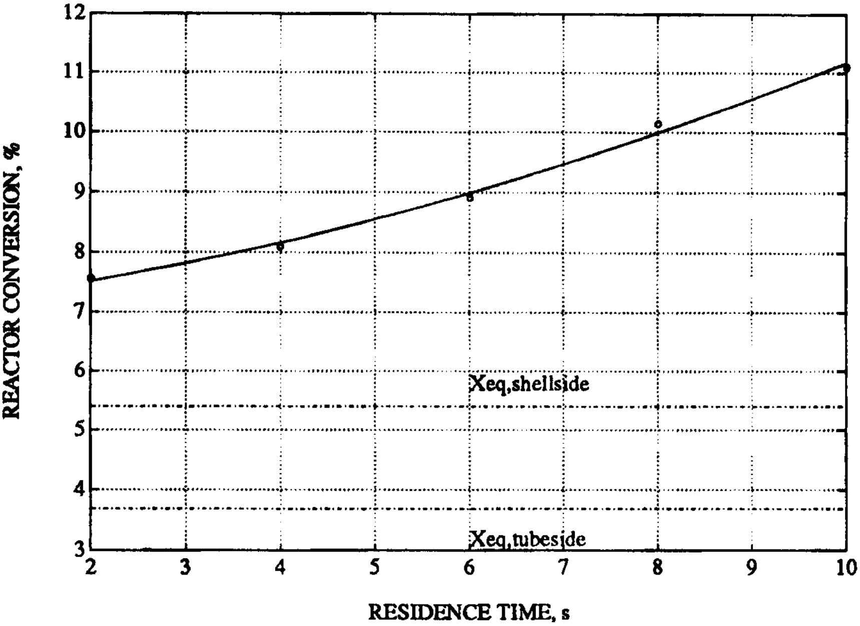

Figure 7: Conversion vs. Residence Time for Dense Feed, T = 550°C, F_r = 1.0, P_o^F = 30 psi, ψ^{PF} = 0.5

reaction rate expressions and to calculate the values of the pertinent kinetic constants. The kinetic experiments were performed in the membrane reactor with the shellside inlet and outlet closed. Detailed descriptions of the kinetic investigations for the ethane dehydrogenation reaction in a CMR have already been published. Detailed kinetic investigations for the ethane PBMR and for the methane steam reforming PBMR go beyond the scope of this conference paper and will be published in future publications. The permeability of all species involved in the reactions were also measured in order to obtain D_{je} values. Experimental details of the permeability measurement technique have already been reported [45,46,62].

For the ethane dehydrogenation reaction in a PBMR, as in the case with the CMR experiments [45], we used two different feed compositions, a dilute feed, con-

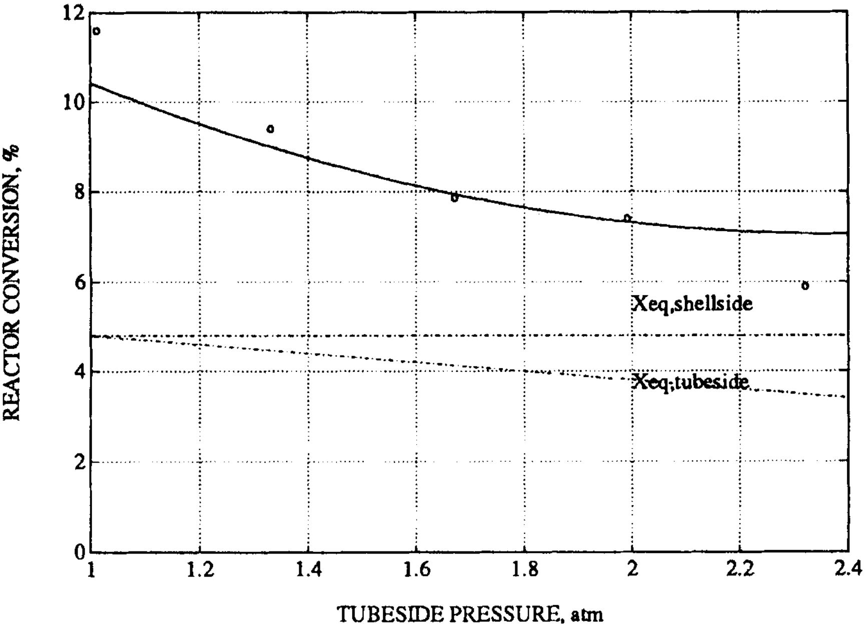

Figure 8: Conversion vs. Pressure for Dense Feed, $F_r = 1.0$, $\tau = 2s$, $T = 550°C$, $\psi^{PF} = 0.5$

sisting of 8.7 mole% ethane, 4.4 mole% hydrogen and 86.9 mole% argon and a dense feed, consisting of 83.4 mole% ethane, 8.3 mole% hydrogen and 8.3 mole% argon. The experiments reported here were carried out in the temperature range of 500-625°C. The selectivity to ethylene was better than 99.9% for temperature less than 575°C and above 98% above this temperature. The effect of sweep rate, feedside residence time, tubeside and shellside pressures and temperature was investigated and detailed extensive accounts can be found elsewhere [62]. The above model was used to fit the data shown (the model results are the solid line) using the thickness of the permselective layer as the only adjustable parameter. Over a broad range of experimental conditions the model performed reasonably well, see for example Figures. 5 and 6 which show the reactor conversion vs. sweep ratio for both the dilute

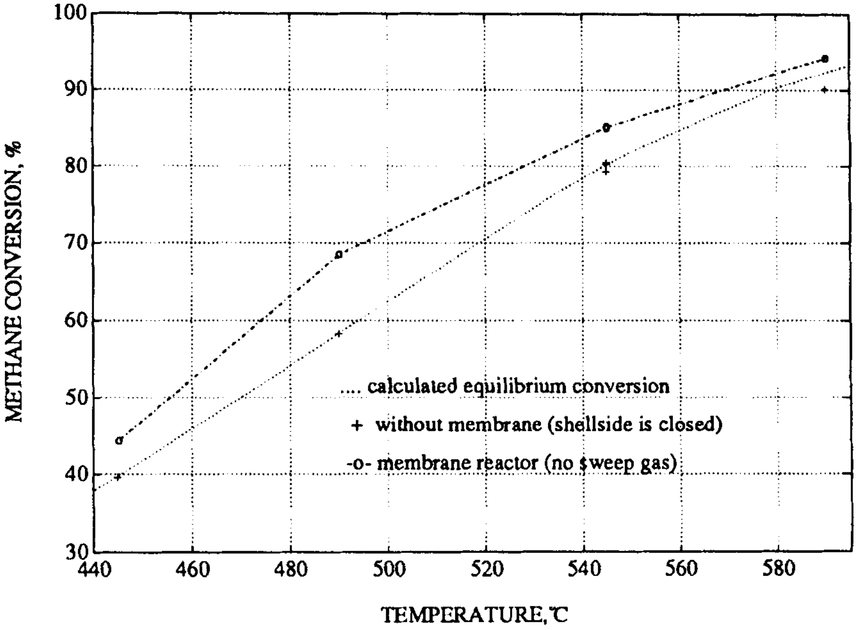

Figure 9: Effect of Membrane Reactor on CH_4 Conversion

and dense feed conditions. The reactor conversion shown in Figure. 6 is already higher than the equlibrium conversion corresponding to either the shellside or tubeside pressure conditions and can be improved further by increasing the residence time or reducing the tubeside pressure, see Figures. 7 and 8.

Finally Figures 9 and 10 show the results of an experiment with the methane steam reforming in a PBMR. Note that under the experimental conditions indicated in these figures, both the overall methane conversion and the conversion to carbon dioxide, indicative of the extent of the water-gas shift reaction, exceed the calculated thermodynamic equlibrium values and the reactor conversion attained in the PBMR with the shellside inlet and outlet closed. The data in Figures 9 and 10 are in the absence of any sweep gas flow in the shellside.

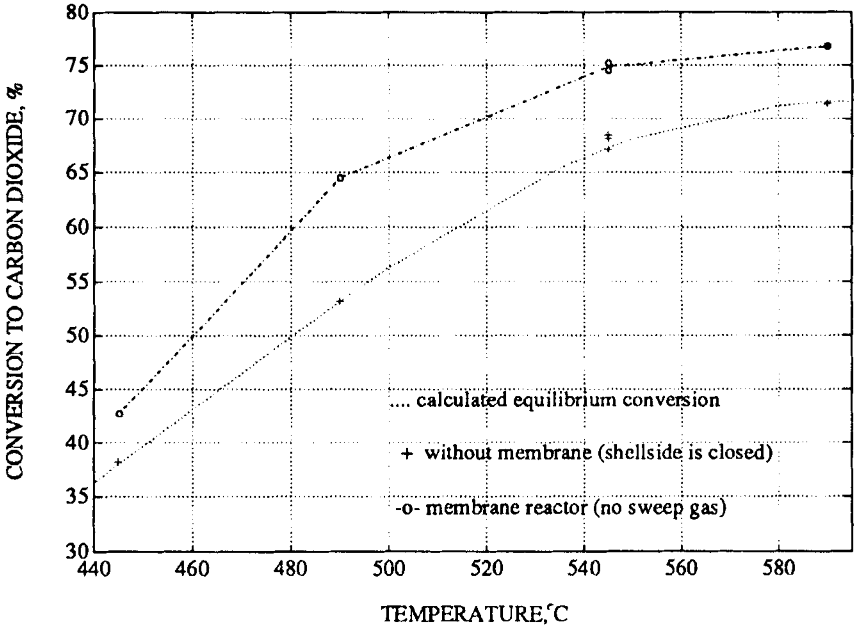

Figure 10: Effect of Membrane Reactor on CO_2 Conversion

CONCLUSIONS

Results have been presented here of membrane reactor studies of the catalytic dehydrogenation of ethane and of the methane steam reforming reactions. A mathematical model for the reactor is also presented, which fits the experimental data reasonably well over a broad range of experimental conditions using only one adjustable parameter, i.e., the thickness of the permselective membrane layer. As mentioned in the introduction, there are many configurations, in which one can operate a membrane reactor. The optimum configuration depends on the reaction, reactor conditions and the membrane characteristics. The choice and design of such reactors is, therefore, aided by a good theoretical model.

LIST OF SYMBOLS

C_j = concentration of species j, moles/m^3

$\mathcal{D}a_i$ = Damkohler number for reaction i

$= \mathcal{D}a_i = \frac{\pi R_1^2 L k_{ri}^F C_{T0}^{\beta_i^f - 1}}{F_0^F}$, dimensionless

D_{je} = effective diffusivity for component j, m^2/s

d_p = equivalent particle diameter, m

f = friction factor

F^F = feed or 'tubeside' volumetric flow rate, m^3/s

F^P = shell or 'shellside' volumetric flow rate, m^3/s

F_r = sweep ratio = $\frac{F_0^P}{F_0^F}$, dimensionless

g_c = conversion factor, if pressure units are in atm.

G^F = (mass flow rate/unit cross section) in the tubeside, g/s.m^2

k_{ri}^F = reaction rate constant in the catalyst bed

$K_{ei}^{\prime F}$ = equilibrium constant in tubeside

K_{ei}^F = equilibrium constant for packed bed = $K_{ei}^{\prime F} C_{To}^{\beta_i^f - \beta_i^r}$, dimensionless

L = length of membrane, m

M_j = molecular weight of component j, gr/gmole

n_j = molar flow rate of component j, moles/sec

n_o^F = total molar flow rate in tubeside, moles/sec

N_{Re} = Reynolds number = $\frac{d_p G}{\mu}$

P_j = partial pressure of component j, atm.

P^F = total pressure in the feed or 'tubeside', atm.

P^P = total pressure in the permeate or 'shellside', atm.

$Q = 2\pi D_{Ae} L / F_0^F$, dimensionless

r = radial distance, m

R = universal gas constant, 82.05 x 10^{-6} m^3 atm/gmole.K

R_1 = inner radius of membrane element, m

R_2 = outer radius of membrane element, m

T = operating temperature, K

$v_j = \frac{M_j}{M_A}$, dimensionless

X_j = mole fraction of component j, dimensionless

$y_j^F = (n_j^F / n_o^F)$, dimensionless

$y_j^P = (n_j^P / n_o^F)$, dimensionless

$Y_j^m = (C_j^m / C_{To}^F)$, dimensionless

z = longitudinal distance, m

Greek Symbols

η_i^F = effectiveness factor for reaction i, dimensionless

$\alpha = \ln(1+\epsilon)$, dimensionless

δ_j = diffusivity ratio = D_{je}/D_{Ae}, dimensionless

$\epsilon = \frac{R_2 - R_1}{R_1}$, dimensionless

ϵ^F = catalyst bed void fraction

ζ = dimensionless length = z/L

ν_{ij} = stoichiometric coefficient of component j for reaction i

μ = gas viscosity, g/m.s

ξ = dimensionless radius = r/R_1

ρ_f = gas density in tubeside, g/m^3

$\psi^{PF} = \frac{P_o^P}{P_o^F}$

$\psi^{P} = \frac{P^P}{P_o^F}$

$\psi^{F} = \frac{P^F}{P_o^F}$

$\omega = \frac{ln\xi}{\alpha}$, dimensionless

Superscripts

F refers to the feed or 'tubeside'

P refers to the permeate or 'shellside'

m refers to the membrane

Subscript

A is the main reactant

i = reaction index

j = component index

T = total

e = effective

o refers to the inlet condition

ACKNOWLEDGEMENT

The support of this research by the Electric Power Research Institute and Medalert Inc. is gratefully acknowledged. We wish also to acknowledge ALCOA for providing us with the Membralox^{TM} membranes and KATALCO Inc. of Chicago, IL for providing the methane steam reforming catalyst. We wish also to thank Drs. Paul K. T. Liu and Ian A. Webster for many helpful discussions.

REFERENCES

1. Williams, T. E., G. Catapano, E. Klein, and R. A. Ward, *AIChE Symp. Ser.*, 268, 85, 1 (1989).
2. Shao, X., S. Xu and R. Govind, *AIChE Symp. Ser.*, 268, 85 (1989).
3. Nazarkina, E. B. and N. A. Kirichenko, *Khim. Tekhnol. Topl. Masel.*,3, 5 (1979).
4. Gryaznov, V. M., L. F. Pavlova, E. Juarez and P. Rivera, *Dokl. Akad. Nauk. SSSR*, 194, 2, 355 (1970).
5. Gur'yanova, O. S., Y. M. Serov, S. G. Gulyanova and V. M. Gryaznov, *Kinet. Katal.*, 29, 4, 850 (1988).
6. Smirnov, V. S., V. M. Gryaznov and A. P. Mishchenko, USSR 256,745 11 Nov 1969, from *Otkrytiya, Izobret., Prom. Obraztsy, Tovarnye Znaki*, 46, 35, 20 (1969).
7. Mikhalenko, N. N., E. V. Khrapova and V. M. Gryaznov, *Neftekhimiya*, 18, 3 (1978).
8. Zhernosek, V. M., N. N. Mikhalenko, S. Iokannes, E. V. Khrapova and V. M. Gryaznov, *Kinet. Katal.*, 20, 4, 921 (1979).
9. Gryaznov, V. M., *Platinum Metals Rev.*, 30, 2 , 68 (1986).
10. Gryaznov, V. M., A. P. Mischenko, V. S. Smirnov, M. E. Sarylova and A. B. Fasman, Br. Pat. Appl. 2,187,756 (1987).
11. Croupnik, G. A. and D. M. Scruggs, US Pat. 4,608,319 (1986).
12. Gryaznov, V. M., V. S. Smirnov, V. M. Vdorin, M. M. Ermilova, L. D. Gogun, N. A. Pritula and I.A. Liininov, Ger. Pat. 2,701,277, 1978; US Pat. 4,132,668 (1979).
13. Gryaznov, V. M., V. S. Smirnov, V. M. Vdorin, M. M. Ermilova, L. D. Gogun, N. A. Pritula and G. K. Fedorova, US Pat. 4,394,294 (1983).

14. Uemiya, S., Y. Kude, K. Suginao, N. Sato, T. Matsuda, and E. Kikuchi, *Chem. Lett.*, 1687 (1988).

15. Uemiya, S., T. Matsuda and E. Kikuchi, *J. Membrane Sci.*, 56, 315 (1991).

16. Kikuchi, E., S. Uemiya, N. Sato, H. Inoue, H. Ando and T. Matsuda, *Chem. Lett.*, 489 (1989).

17. Uemiya, S, N. Sato, H. Ando, and E. Kikuchi, *Ind. & Eng. Chem. Res.*, 30, 3, 585-589 (1991).

18. Uemiya, S, N. Sato, H. Ando, T. Matsuda and E. Kikuchi, *Appl. Catal.*, 67, 223 (1991).

19. Uemiya, S, N. Sato, H. Ando, T. Matsuda and E. Kikuchi, *Sekiyu Gakkaishi*, 33, 418 (1990).

20. Uemiya, S., T. Matsuda and E. Kikuchi, *Chem. Lett.*, 8, 1335 (1990).

21. Omata, K., S. Hashimoto, H. Tominaga and K. Fujimoto, *Appl. Catal.*, 52, L1 (1989).

22. Etsel, T. H. and S. M. Flengas, *J. Electrochem. Soc.*, 118, 1890 (1971).

23. Weissbart, J., W. H. Smart and T. Wyderen, *Aerospace Med.*, 40, 136 (1969).

24. Nigara, Y. and B. Cales, *Bull. Chem. Soc. Jpn.*, 59, 1997 (1986).

25. Cales, B. and J. F. Baumard, *High Temp. High Pressures*, 14, 681 (1982).

26. Pancharatnam, S., R. A. Huggins and D. M. Mason, *J. Electrochem. Soc.*, 122, 869 (1975).

27. Stoukides, M. and C. G. Vayenas, *J. Catal.*, 70, 137 (1981).

28. Vayenas, C. G. and R. D. Farr, *Science*, 208, 593 (1980).

29. Farr, R. D. and C. G. Vayenas, *J. Electrochem. Soc.*, 127, 7, 1478 (1980).

30. Michaels, J. N. and C. G. Vayenas, *J. Cat.*, 85, 477 (1984).

31. Stoukides, M. and C. G. Vayenas, *J. Electrochem. Soc.*, 131, 840 (1984).

32. Gür, T. M. and R. A. Huggins, *Science*, 219, 967 (1983).

33. Gür, T. M. and R. A. Huggins, *J. Cat.*, 102, 443 (1986).

34. Otsuka, K., S. Yokogama and A. Morikawa, *Bull. Chem. Soc. Jpn.*, 57, 3286 (1984).

35. Otsuka, K., S. Yokogama and A. Morikawa, *Chem. Lett.*, 319 (1985).

36. Hazburn, E. A., US Pat. 4,791,079 (1988).

37. Dicosimo, R., J. D. Barrington and R. K. Grasseli, US Pat. 4,571,443 (1986).

38. Ryu, J., B. Morriseau and V. Jalan, Paper presented at the 4th NAMS Meeting, San Diego, CA, May 1991.

39. Gryaznov, V. M., V. I. Vedernikov and S. G. Gulyanova, *Kinet. Katal.*, 27, 142 (1986).

40. Kameyama, T., M. Dokiya, M. Fujishige, H. Yokokama and K. Fukuda, *I&EC Fund.*, 20, 97 (1981).

41. Itoh, N., Y. Shindo, K. Haraya, and T. Hakuta, *Sekiyu Gakkaishi*, 32, 1, 47 (1989).

42. Itoh, N., Y. Shindo, K. Haraya, and T. J. Hakuta, *Chem. Eng. Jpn.*, 21, 4, 399 (1988).

43. Nagamoto, H. and H. Inoue, *Chem. Eng. Commun.*, 34, 315 (1985).

44. Wu, J. C. S., T. E. Gerdes, J. L. Pszczolkowski, R. R. Bhave and P. K. T. Liu, *Sepn. Sci. Tech.*, 25, 1489 (1990).

45. Champagnie, A. M., T. T. Tsotsis, R. G. Minet and I. A. Webster, *Chem. Eng. Sci.*, 45, 8, 2423-2429 (1990).

46. Champagnie, A. M., T. T. Tsotsis, R. G. Minet and E. Wagner,*J. Catal.*, 134, 713 (1992).

47. Minet, R. G., and T. T. Tsotsis, U. S. Pat. 4,981,676 A (1991).

48. Zaspalis, V. T., Ph.D. Thesis, University of Tuente, The Netherlands, Nov. 1990.

49. Okubo, T., K. Haruta, K. Kusakabe, S. Morooka, H. Anzai, and S. Akiyama. *Ind. Eng. Chem. Res.*, 30, 4, 614 (1991).

50. Zaspalis, V. T., W. van Praag, K. Keizer, J. G. van Ommen, J. R. H. Ross and A. J. Burgraaf, *Appl. Catal.*, 74, 205 (1991).

51. Zaspalis, V. T., W. van Praag, K. Keizer, J. G. van Ommen, J. R. H. Ross and A. J. Burgraaf, *Appl. Catal.*, 74, 223 (1991).

52. Zaspalis, V. T., W. van Praag, K. Keizer, J. G. van Ommen, J. R. H. Ross and A. J. Burgraaf, *Appl. Catal.*, 74, 235 (1991).

53. Davidson, A. P. and M. Salim, *British Ceram. Proc.*, 43, 119 (1988).

54. Tsotsis, T. T., N. Nourbarkhsh, and I. A. Webster, *Prep. - Am. Chem. Soc., Div. Pet. Chem.*, 33, 502 (1989).

55. Tsotsis, T. T., N. Nourbarkhsh, A. M. Champagnie and I. A. Webster, *AIChE Symp. Ser.*, 286, 78 (1989).

56. Bitter, J. G. A., Br. Pat. GB 2,201,159 (1988).

57. Ma, Y. H., Y. L. Becker, W. R. Moser and A. G. Dixon, *Proc. 2nd Int. Conf. on Inorganic Membranes,* 61, 62, pp. 337, Montpellier France, July 1-4, 1991.

58. Vora, B. V., P. R. Pujado, and R. F. Anderson, *Energy Prog.*, 6, 3, 171 (1986).

59. Xu, J. and G. F. Froment, *AIChE J.*, 35, 88 (1989).

60. Oertel, M., J. Schmitz, W. Welrich, D. J. Neumann and R. Schulten, *Chem. Eng. Technol.*, 10, 248 (1987).

61. Adris, A. M., S. S. E. H. Elnashaie and R. Hughes, In Press, *Can. J. Chem. Eng.*, 69, 1061 (1991).

62. Champagnie, A. M., Ph.D. Thesis, University of Southern California, Los Angeles, CA, 1991.